Journal of Applied Polymer Science

The synthesis and characteristics of sodium alginate/graphene oxide composite films crosslinked with multivalent cations

Haicheng Zheng, Jisheng Yang, Suya Han
College of Chemistry and Chemical Engineering, Yangzhou University, Yangzhou 225002, China
Correspondence to: J. Yang (E-mail: jsyang@yzu.edu.cn)

ABSTRACT: Association of a method of the incorporation of graphene oxide (GO) into sodium alginate (Na-alg) polymer matrix with a method of the use multivalent cations crosslinker was put forward to synthesize novel Na-alg/GO nanocomposite films. The structures, morphologies, and the properties of Na-alg/GO films were characterized by Fourier transform infrared (FTIR) spectroscopy, X-ray diffraction (XRD), field-emission scanning electron microscopy (FE-SEM), thermogravimetric analysis (TGA), and tensile tests. The results revealed that the interlayer distance of GO sheets increased from 0.83 nm to 1.08 nm after assembling with Na-alg, and Na-alg inserted into GO layers crosslinking with multivalent cations increased the interlayer distance further. Ionic crosslinking significantly enhanced thermal and mechanical properties of Na-alg/GO nanocomposite films. In particular, Fe^{3+} led to Na-alg/GO nanocomposite films of significantly higher tensile strength and modulus than Ca^{2+} and Ba^{2+}. The excellent thermal and mechanical properties of these novel Na-alg/GO nanocomposite films may open up applications for Na-alg films. © 2016 Wiley Periodicals, Inc. J. Appl. Polym. Sci. **2016**, *133*, 43616.

KEYWORDS: composites; crosslinking; films; properties and characterization

Received 4 November 2015; accepted 4 March 2016
DOI: 10.1002/app.43616

INTRODUCTION

Sodium alginate (Na-alg) is a linear anionic natural polysaccharide composing of 1,4-linked residues of β-D-mannuronic (M) acid and α-L-guluronic acid (G) at different proportions in the chain.[1] Over the past few years, it as a star in biomaterials research has been attracting tremendous attention in various fields.[2] It is being developed for diverse applications, including tissue engineering,[3] drug delivery,[4–6] and wound dressings,[7] due to its biocompatibility, low toxicity, relatively low cost, and functional gelation by addition of multivalent cations. The Na-alg itself, however, displays some unsatisfactory properties such as poor mechanical strength, low-stretch properties, and loss of structural integrity badly restricted its practical applications.[8] Thus, an effective approach for improving the situation is necessary.

More recently, great interest has been focused on developing novel Na-alg with improved mechanical properties. As a successful example, nanocomposite Na-alg with unique structures and high mechanical strength which are composed of Na-alg and inorganic nanofillers, such as clays,[9] carbon nanotubes,[10] halloysite nanotubes,[3] and graphene oxide (GO)[11] have been put forward. Nowadays, GO has been no doubt the hottest topic due to its excellent optical, electrical, mechanical properties, and unique flat structure with atomic thickness.[12] The low costs and mass production of GO which possesses abundant oxygen-containing groups for further functionalization have been realized. Apart from this, it's good dispersibility in water is also attracted by scientists.[13] Ordinarily, a small quantity of GO sheet is used as physical filler to improve the mechanical properties of the polymer substrates.[14] Besides these, multivalent ions can also induce the assembly of a GO through strong coordinations with carboxylic groups at the edges of GO sheets and weak binding with the epoxy and carbonyl groups on the GO planes.

Na-alg is hydrophilic and soluble matrix. However, it can form crosslink networks through ionic interactions with multivalent cations (e.g., Ca^{2+}, Ba^{2+}, and Fe^{3+}) and the crosslinking process with polyvalent cations has been used to improve their water resistance, mechanical resistance, barrier properties, cohesiveness, and rigidity.[15,16] Moreover, the crosslinking process and properties of Na-alginate are strongly dependent on the kinds of cations and the method used for the introduction of the crosslinking ions.

Incorporation of GO on Na-alg and the use of multivalent cations crosslink had been both reported in literature. The novelty of this article was the association of these methods. The properties of Na-alg/GO nanocomposite films were greatly enhanced after the films crosslinked with multivalent cations. Specially,

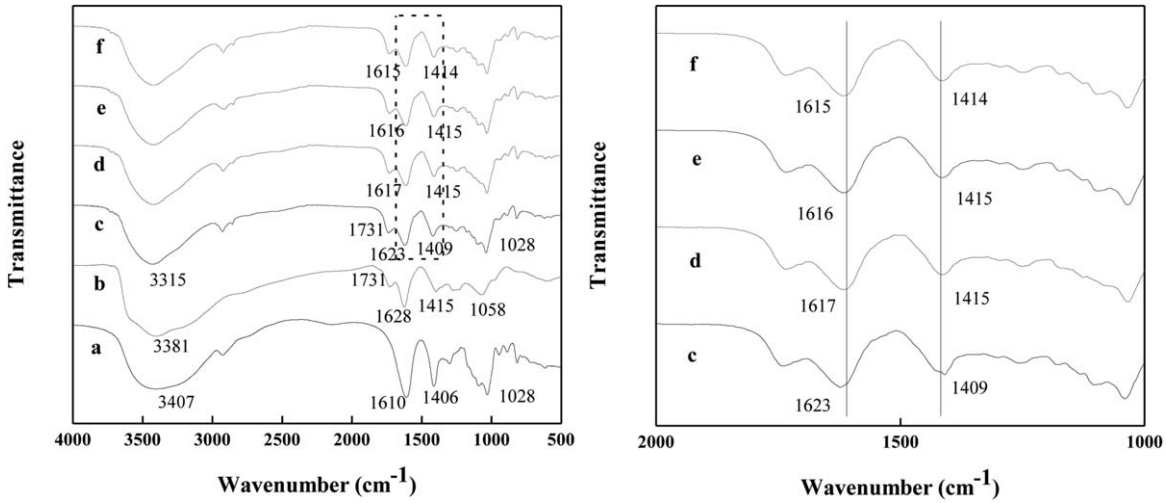

Figure 1. Left: FTIR spectra of (a) Na-alg, (b) GO, (c) Na-alg/GO, (d) Ca-alg/GO, (e) Ba-alg/GO, and (f) Fe-alg/GO. Right: Magnified FTIR spectra of dashed box in left.

the Na-alg/GO nanocomposite films crosslinked with Fe^{3+} cations were much excellent than those crosslinked with Ca^{2+} and Ba^{2+} cations. We supposed that these Na-alg/GO nanocomposite films with excellent properties will open up applications, such as structural materials.

EXPERIMENTAL

Materials

Sodium alginate (Na-alg), natural graphite powders were bought from Qingdao Huatai lubricant sealing S&T Co. Ltd. (Qingdao, Chain). $CaCl_2$, $BaCl_2$, $FeCl_3$ were bought from Sinopharm Chemical Reagent Co. Ltd. (Shanghai, China). All materials were used without further purification. Distilled water was used for the preparation of all solutions.

Synthesis of Na-alg/GO Films Crosslinked with Multivalent Cations

GO was synthesized by the modified Hummer's method.[17] Briefly, graphite powder (1.0 g) was oxidized in 20.0 mL mixture of HNO_3 and H_2SO_4 (1:3, vol/vol) under reflux for 2 days. The preoxidized graphite was separated by centrifugation, washed with dry THF and dried under vacuum. The preoxidized graphite was further oxidized by a mixture of 96% H_2SO_4 (40.0 mL) and $KMnO_4$ (5.0 g). At the end, the GO was collected and dried under vacuum. The Na-alg/GO composite films crosslinked with multivalent cations were synthesized by a two-step method. In the first step, Na-alg polymer (2 g) was dissolved in 100 mL of deionized water, and then 15 mL of GO (4 mg/mL) suspension was added into the Na-alg solution. After constantly stirred for 1 h at 25 °C using a magnetic stirrer, the mixture was transferred into a mold (150.0 mm × 150.0 mm × 2.0 mm), after that, the mold was put in an oven at 60 °C for 12 h to get Na-alg/GO nanocomposite film. Second, after peeled off from the mold, Na-alg/GO films were soaked in a 0.3 *M* aqueous solution of multivalent cations (Ca^{2+}, Ba^{2+}, Fe^{3+}) at room temperature for 6 h to form the novel Na-alg/GO nanocomposite films.

Characterization

To research possible interactions in the Na-alg/GO films crosslinked with multivalent cations, Fourier transform infrared spectroscopy (FTIR, Tensor 27, Germany) was performed with record between 4000 and 500 cm^{-1}. X-ray diffraction was used, with a D8 Advance Superspeed X-ray diffraction (X-ray, Germany) with Cu as anode target ($\lambda = 0.15406$ nm), pipe voltage of 40 kV, flow of 200 mA to analyze the distribution of GO in alginate matrix, and the influence of ion crosslinking agent. The measurements were carried out in the 2θ range of 3°–60°. Field-emission scanning electron microscopy (FE-SEM) images were obtained using a S4800 at an acceleration voltage of 15.0 kV. Thermo gravimetric analysis (TGA, STA409PC, Germany) in a nitrogenous atmosphere was used to research the thermal stability of nanocomposite films.

Mechanical test was performed using a universal mechanical test (Instron, Model 3382, USA) at a speed of 2 mm/min at room temperature and relative humidity was 45–50%. For each sample, a minimum of ten measurements was taken, and the average result was calculated.

RESULTS AND DISCUSSION

FTIR Studies

Figure 1 shows the absorption bands from FTIR spectrum of Na-alg, GO, M-alg/GO (M = Na, Ca, Ba, Fe). The right figure is the A zoomed in view of the dashed box. For native Na-alg spectrum, 3407 cm^{-1}, 1610 cm^{-1}, 1406 cm^{-1}, and 1028 cm^{-1} were assigned to OH stretching vibration, symmetric and asymmetric COO^- stretching vibration of carboxylate salt group, and stretching vibration of C—O—C groups, respectively.[18] In the GO spectrum, the peak at 3381 cm^{-1} was attributed to OH stretching vibration, the band at 1731 cm^{-1} corresponded to C=O stretching vibration of the carboxylic group, and dominant peaks appeared at 1628 cm^{-1} and 1058 cm^{-1}, which were typical of aromatic C=C and symmetric C—O stretching in the C—O—C group, respectively.[19]

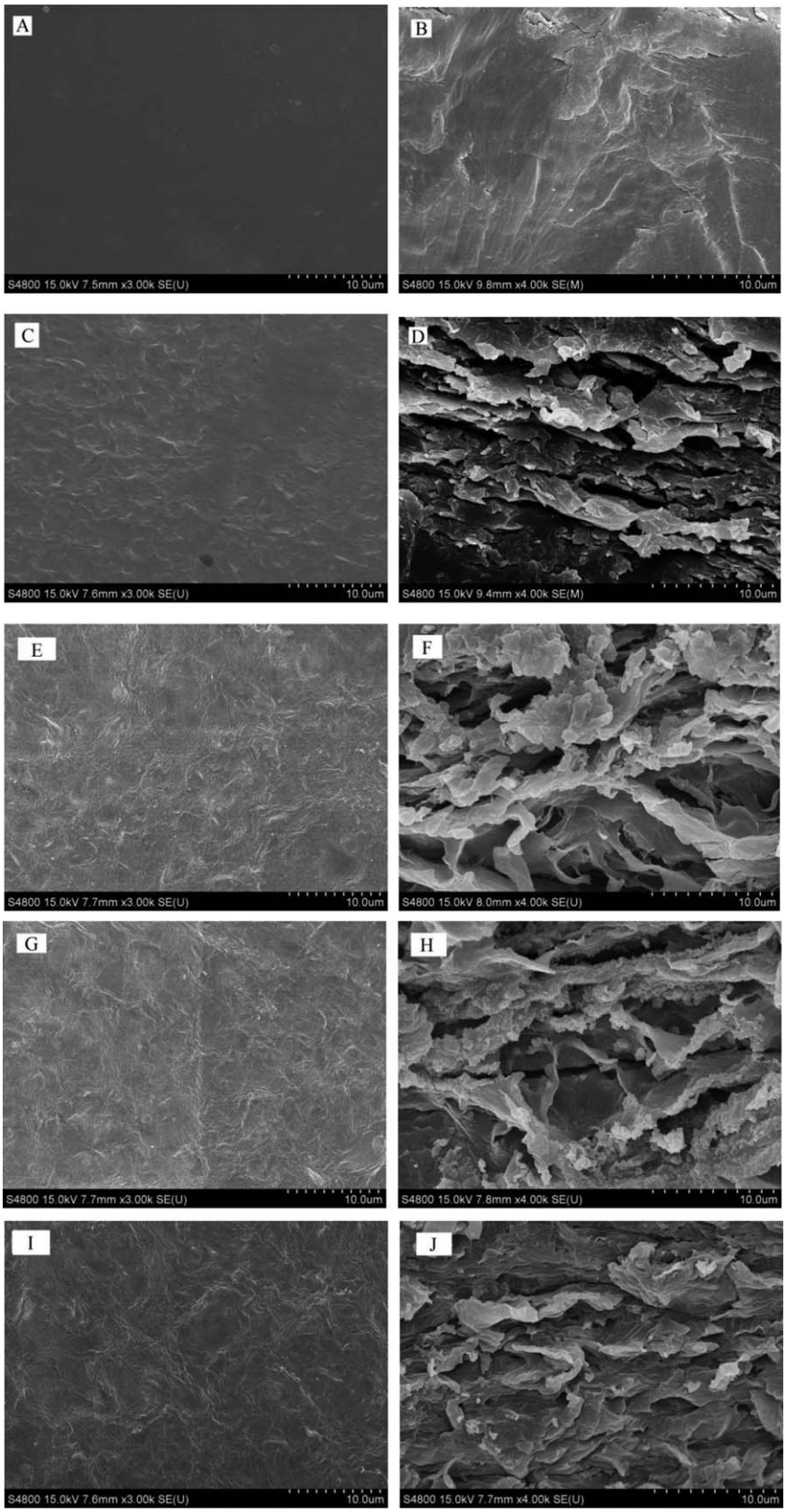

Figure 2. SEM surface images (A,C,E,G,I) and fracture surface images (B,D,F,H,J) of Na-alg (A,B), Na-alg/GO (C,D), Ca-alg/GO (E,F), Ba-alg/GO (G,H), and Fe-alg/GO (I,J).

The FTIR spectrum of Na-alg/GO nanocomposite films demonstrated characteristic peaks of both Na-alg chains and GO sheets. A peak at 1731 cm^{-1} due to the C═O stretching vibration of the carboxylic group from the GO could be observed. Furthermore, compared the peaks at 3407 cm^{-1} [Figure 1(a)] and 3381 cm^{-1} [Figure 1(b)], the peak at 3315 cm^{-1} in Na-alg/GO attributed to OH stretching vibration broadened and shifted to smaller wavelengths [Figure 1(c)]. This phenomenon in the FTIR spectra adequately revealed that Na-alg and GO in the Na-alg/GO nanocomposite films were intertwined via strong hydrogen-bonding interactions between oxygen-containing group of GO sheets and Na-alg chains.

For Na-alg/GO nanocomposite films, the peak at 1623 cm^{-1} and somewhat weaker peak at 1409 cm^{-1} were attributed to the asymmetric and symmetric stretching vibration of the carboxylate group, respectively. These two peaks (1623 cm^{-1} and 1409 cm^{-1}) were the most useful characteristic peaks to investigate the ion crosslinking or exchange process. As seen in Figure 1(d–f) of right figure, it is evident that when the Na-alg and GO were crosslinked with Ca^{2+}, Ba^{2+}, and Fe^{3+}, the symmetric COO^- peak shifted to a higher wavenumbers (from 1409 to 1415, 1415, and 1414 cm^{-1}) and the asymmetric COO^- peak shifted to a low wavenumbers (from 1623 to 1617, 1616, and 1615 cm^{-1}). As calcium, barium, and ferric ions in the alginate blocks the charge densities were changed, creating new environments around the carboxylate group.[20] These could be resulted from a strong interaction between the carboxylate group and multivalent cation, as a result of the crosslinking.

SEM Analysis

SEM measurements provided direct information regarding the interfacial interactions and crosslinking of M-alg/GO nanocomposite films. As shown in Figure 2(A), the surface of the pure Na-alg was smooth, whereas there were some salient banded structures on the surface of Na-alg/GO [Figure 2(C)]. The distinction might be attributed to the GO sheets embedded into Na-alg matrix. As shown in Figure 2(B,D), there was significant difference between them. Compared with the cross-section of the pristine Na-alg, a layered structure caused by the incorporation of GO could be clearly observed in the cross-section of the Na-alg/GO composites. Figure 2(E,G,I) shows the surface SEM micrographs of Na-alg/GO composites crosslinked with Ca^{2+}, Ba^{2+}, and Fe^{3+} cations, respectively. The surfaces of the M-alg/GO (M = Ca, Ba, and Fe) were totally different from that of the Na-alg/GO, which were probably due to the multivalent cations crosslinked alginate by simultaneously associating with carboxylic groups on different units of alginate chains. Additionally, there was no obvious difference on the surface from the M-alg/GO. As indicated in Figure 2(D,F,H,J), the inner structures of M-alg/GO were much denser than those of Na-alg/GO, which predicted the enhancement of the tensile strength. Multivalent cations could crosslink the Na-alg so as to change the assembling structures of Na-alg, resulting in the aggregation of the polymer chains. In addition, oxygen functional groups on the basal planes of the GO sheets and the carboxylate groups on the edges could both bond to Ca^{2+}, Ba^{2+}, and Fe^{3+}.[21] All these differences might be attributed to the interactions including hydrogen bonding, electrostatic interaction, and interfacial interaction.

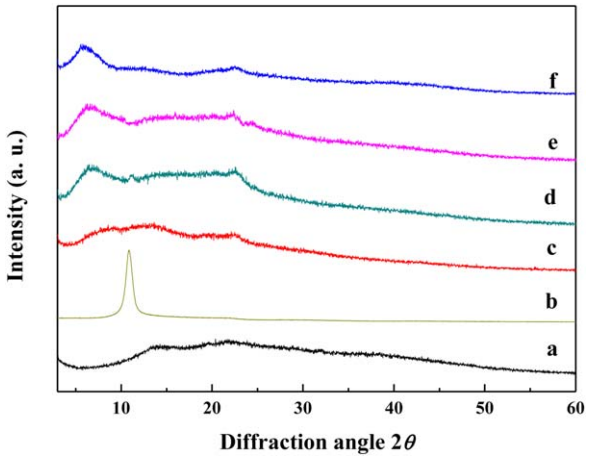

Figure 3. XRD patterns of (a) Na-alg, (b) GO, (c) Na-alg/GO, (d) Ca-alg/GO, (e) Ba-alg/GO, and (f) Fe-alg/GO. [Color figure can be viewed in the online issue, which is available at wileyonlinelibrary.com.]

XRD Discussions

To further reveal the microstructures of the Na-alg/GO nanocomposite films, X-ray diffraction (XRD) patterns were obtained on Na-alg, GO, M-alg/GO nanocomposite films. The XRD pattern of Na-alg presented two weak and broad diffractions at 14.0° and 22.1° indicating a rather amorphous structure [Figure 3(a)]. As demonstrated in Figure 3(b), the pattern of GO exhibited a characteristic peak at $2\theta = 10.7°$, which meant the interlayer spacing of the GO nanosheets was 0.83 nm. Na-alg/GO nanocomposite film presented three peaks at 8.2°, 14.0°, and 22.1°, the former peak associated with GO and the latter two peaks corresponded to Na-alg. The diffraction angle characteristic for GO shifted from 10.7° to 8.2°, which revealed that the interlayer spacing of GO increased from 0.83 nm to 1.08 nm. The information demonstrated that the Na-alg molecules inserted into the interlayer of GO forming the intercalated structures. After crosslinking with Ca^{2+}, Ba^{2+}, as shown in Figure 3(d,e), the XRD patterns presented diffraction peaks at 6.7° and 6.5° associated with GO, respectively. The peak at 5.8° corresponded to GO shifted toward lower angle value further and the GO interlayer spacing increased after crosslinking with Fe^{3+} [Figure 3(f)]. Ca^{2+}, Ba^{2+}, and Fe^{3+} permeated into the interlayer of GO[22] and then crosslinked with Na-alg resulting in a larger aggregate, these might be the reason that the GO interlayer spacing increased. In particular, compared the XRD pattern of Ca-alg/GO and Ba-alg/GO with Fe-alg/GO, the peak of GO in Fe-alg/GO (5.8°) was lowest than that in Ca-alg/GO (6.7°) and Ba-alg/GO (6.5°). The properties of the crosslinker ions decided crosslinking degree of Na-alg. Fe^{3+} could interact with three carboxylic groups of different alginate chains at the same time, resulting in a more compact structure.[23] Nevertheless, for Ca^{2+} and Ba^{2+}, egg box model illustrated the cooperative binding of calcium ions between two Na-alg chains.[24]

On the basis of FTIR, SEM, and XRD analysis, the schematic illustrations in Scheme 1 displayed the vivid models for the Na-

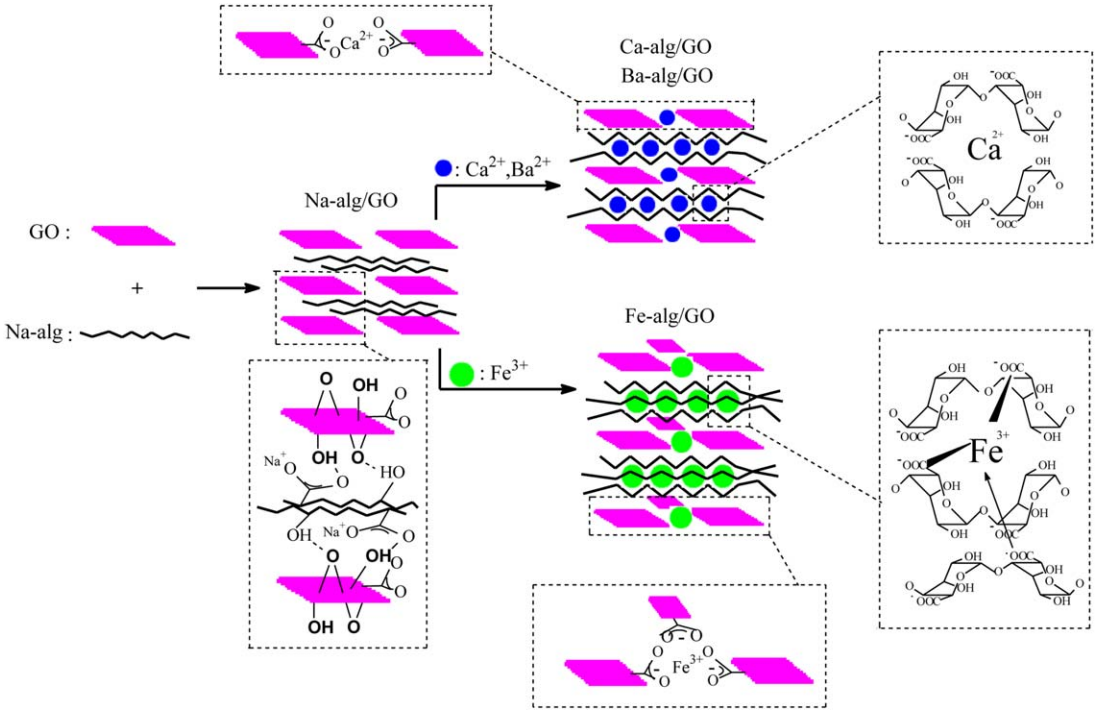

Scheme 1. Schematic models of the alginate/GO composite films crosslinked by multivalent cations. [Color figure can be viewed in the online issue, which is available at wileyonlinelibrary.com.]

alg/GO nanocomposite films crosslinked with multivalent cations. The formations of these nanocomposite films were under the synergistic effects of three types of interactions: hydrogen bonds between GO sheets and alginate chains, multivalent cations induced algiante network, and multivalent cations interacted with GO sheets.

Thermal Degradation Behaviors

We compared the thermal properties of Na-alg, Na-alg/GO, and M-alg/GO nanocomposite films and the TGA and DTG curves are shown in Figures 4 and 5, respectively. It could be observed that all the samples had the first weight loss around 87.5 °C which was attributed to the loss of adsorbed moisture from the film.[25] From the second weight loss of Na-alg and Na-alg/GO, we could conclude that the thermal stability of Na-alg film increased with the addition of GO which revealed that there was hydrogen-bonding interactions between oxygen-containing group of GO sheets and Na-alg chains. The temperatures of starting thermal degradation of M-alg/GO were lower than Na-alg/GO, while they needed higher temperatures than Na-alg/GO to completely degrade thermally. As seen in Figure 4, Fe-alg/GO possessed lower thermal stability. Carbon covalence dissociated into carbon free radical which would react with Fe^{3+} when the system reached a certain temperature. During this stage, the fracture of glycosidic bonds, dehydration, and decarbonylation of alginate occurred, leading to the releases of CO_2, H_2O, and other small

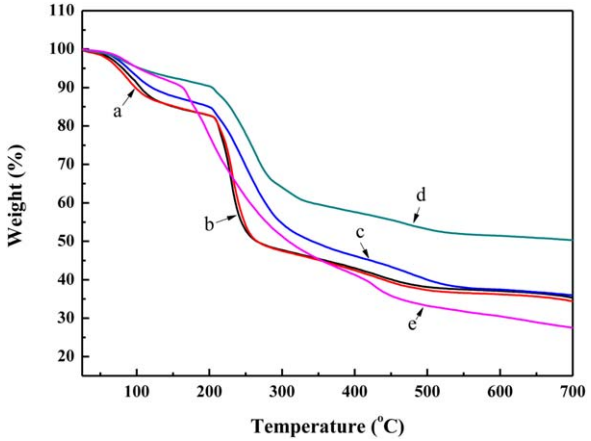

Figure 4. TGA curves of (a) Na-alg, (b) Na-alg/GO, (C) Ca-alg/GO, (d) Ba-alg/GO, (e) Fe-alg/GO. [Color figure can be viewed in the online issue, which is available at wileyonlinelibrary.com.]

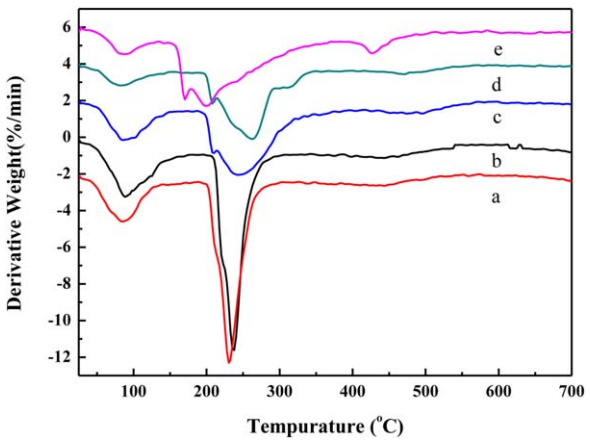

Figure 5. DTA curves of (a) Na-alg, (b) Na-alg/GO, (C) Ca-alg/GO, (d) Ba-alg/GO, (e) Fe-alg/GO. [Color figure can be viewed in the online issue, which is available at wileyonlinelibrary.com.]

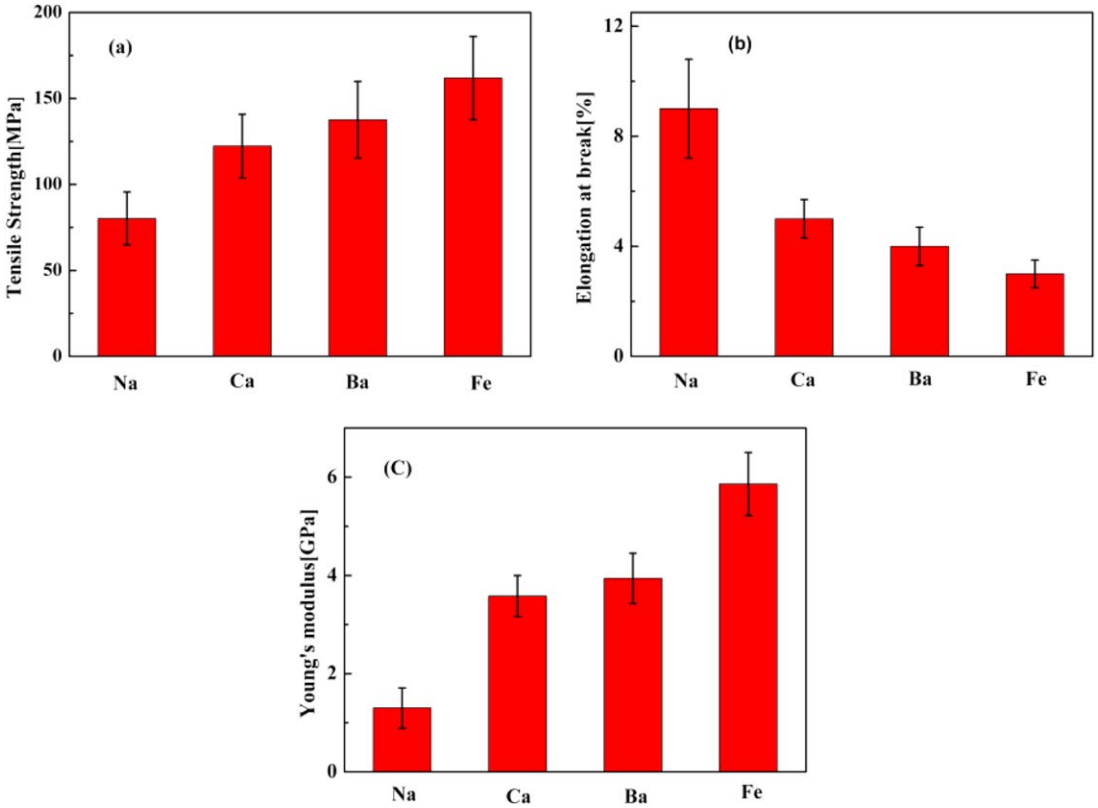

Figure 6. Tensile strength (a), elongation at break (b), and Youngs' modulus (c) of M-alg/GO composite films. Error bars show standard deviation. [Color figure can be viewed in the online issue, which is available at wileyonlinelibrary.com.]

weight molecules.[26] Thermal property of polymer greatly depended on the chain mobility of the macromolecules which was ultimately affected by the factors such as intra- or intermolecular forces, crosslinking density, etc.[27] Na-alg and GO could both crosslink with multivalent cations resulting in the improvement of thermal stability of Na-alg/GO nanocomposite films

Mechanical Properties Investigation

Eventually, the mechanical behaviors of the M-alg/GO nanocomposite films were investigated by tensile tests and the results are presented in Figure 6. The data were the average results measured for 10 samples. Na-alg/GO showed low strength (80.2 ± 15.4 MPa) and elastic modulus (1.30 ± 0.41 GPa) that was higher than Na-alg (tensile strength 33.6 MPa) and Ca-alg (3 g/100 mL $CaCl_2$ tensile strength strength 73.3MPa) in the literature.[28] As expected, Fe-alg/GO nanocomposite film reached tensile strength of 161.8 ± 24.2 MPa and elastic modulus of 5.86 ± 0.64 GPa, Ba-alg/GO and Ca-alg/GO nanocomposite films reached tensile strength of 137.6 ± 22.3 MPa and 122.3 ± 18.5 MPa and elastic modulus of 3.94 ± 0.51 GPa and 3.58 ± 0.42 GPa, respectively. In addition, the elongations at break of Na-alg/GO nanocomposite films were lower than M-alg/GO which agreed with the work by Russo *et al.*[29]

The monovalent Na^+ cations did not crosslink alginate chains, whereas multivalent cations crosslinked alginate by simultaneously associating with carboxylic groups on different units of alginate chains. In addition, multivalent ions induced the assembly of a GO through strong co-ordinations with carboxylic groups at the edges of GO sheets and weak binding with the epoxy and carbonyl groups on the GO planes.[21] Alginate network intertwined with GO sheets by the bridging of hydrogen-bond interactions, thus resulting in an integrated and stable network.

Deramos *et al.* reported that the interactions between multivalent cations and Na-alg depended on the charge and ion radius.[30] Compared with Ba^{2+} and Ca^{2+}, Fe^{3+} could interact with three carboxylic groups of different alginate chains at the same time, forming a more compact network.[23] Accordingly, Fe-alg/GO nanocomposite film exhibited higher mechanical properties. As for divalent cations, Ba^{2+} (1.35 Å) were expected to fill a larger space between the blocks of Na-alg polymers, resulting in a tighter arrangement of crosslinked alginate polymers than Ca^{2+} (1.0 Å).

CONCLUSIONS

In summary, the novel M-alg/GO nanocomposite films possessing excellent mechanical properties were successfully synthesized by a facile two-step strategy. First, the Na-alg/GO nanocomposite films were prepared by assembly, and then were immersed in aqueous solutions containing Fe^{3+}, Ba^{2+}, and Ca^{2+}. Hydrogen bond and interfacial adhesion induced the self-assembly of Na-alg and GO. After assembled with Na-alg, the interlayer spacing of GO sheets increased from 0.83 nm to 1.08 nm. When Na-alg/GO composite films were crosslinked with multivalent cations, the interlayer spacing of GO sheets increased further. From the thermal degradation analysis, it could be observed that the thermal stability of M-alg/GO was higher than Na-alg/GO. Ionic crosslinking of alginate regulated by a convenient ion-exchange

approach, hydrogen bonds between GO sheets and Na-alg chains and interactions between multivalent cations and GO resulted in the composite films of high tensile strength. In particular, we discovered that the Fe-alg/GO composite films were much stronger than Na-alg/GO crosslinked by divalent cations. There is no doubt that these novel nanocomposite films are expected to be used in packing materials and structural materials.

ACKNOWLEDGMENTS

Authors gratefully acknowledge the financial support from a project funded by the Priority Academic Program Development of Jiangsu Higher Education Institutions, Natural Science Foundation of Yangzhou (yz2014066), and the devices support from testing center of Yangzhou University.

REFERENCES

1. Yang, J. S.; Zheng, H. C.; Han, S. Y.; Jiang, Z. D.; Chen, X. *RSC Adv.* **2015**, *5*, 2378.
2. Yang, J. S.; Han, S. Y.; Zheng, H. C.; Dong, H. B.; Liu, J. B. *Carbohydr. Polym.* **2015**, *123*, 53.
3. Liu, M. X.; Dai, L. B.; Shi, H. Z.; Xiong, S.; Zhou, C. R. *Mater. Sci. Eng., C* **2015**, *49*, 700.
4. Strasdat, B.; Bunjes, H. *Int. J. Pharm.* **2015**, *489*, 203.
5. Wu, J.; Kong, T. T.; Yeung, K. W. K.; Shum, H. C.; Cheung, K. M. C.; Wang, L. Q.; To, M. K. T. *Acta Biomater.* **2013**, *9*, 7410.
6. Calija, B.; Cekic, N.; Savic, S.; Danielsc, R.; Markovic, B.; Milic, J. *Colloid Surf. B* **2013**, *110*, 395.
7. Thu, H. E.; Zulfakar, M. H.; Ng, S. F. *Int. J. Pharm.* **2012**, *434*, 375.
8. Abdollahi, M.; Alboofetileh, M.; Rezaei, M.; Behrooz, R. *Food Hydrocoll.* **2013**, *32*, 416.
9. Alboofetileh, M.; Rezaei, M.; Hosseini, H.; Abdollahi, M. *J. Food Eng.* **2013**, *117*, 26.
10. Yan, L. Y.; Chen, H. L.; Li, P.; Kim, D. H.; Chan-Park, M. B. *ACS Appl. Mater. Interface* **2012**, *4*, 4610.
11. Nie, L.; Liu, C. H.; Wang, J.; Shuai, Y.; Cui, X. Y.; Liu, L. *Carbohydr. Polym.* **2015**, *117*, 616.
12. Huang, X.; Qi, X. Y.; Boey, F.; Zhang, H. *Chem. Soc. Rev.* **2012**, *41*, 666.
13. Xu, Y. X.; Sheng, K. X.; Li, C.; Shi, G. Q. *ACS Nano* **2010**, *4*, 4324.
14. Cong, H. P.; Wang, P.; Yu, S. H. *Small* **2014**, *10*, 448.
15. Crossingham, Y. J.; Kerr, P. G.; Kennedy, R. A. *Int. J. Pharm.* **2014**, *473*, 259.
16. Kilan, K.; Warszynski, P. *Electrochim. Acta* **2014**, *144*, 254.
17. Xu, Y. X.; Bai, H.; Lu, G. W.; Li, C.; Shi, G. Q. *J. Am. Chem. Soc.* **2008**, *130*, 5856.
18. Luo, Y. X.; Lode, A.; Wu, C. T.; Chang, J.; Gelinsky, M. *ACS Appl. Mater. Interface* **2015**, *7*, 6541.
19. Li, Y. Q.; Trung, D. Y.; Chen, S. B.; Wang, Q. H.; Pan, G. Q.; Wang, T. M. *Mater. Des.* **2013**, *47*, 850.
20. Li, J. W.; He, J. M.; Huang, Y. D.; Li, D. L.; Chen, X. T. *Carbohydr. Polym.* **2015**, *123*, 208.
21. Park, S.; Lee, K. S.; Bozoklu, G.; Cai, W. W.; Nguyen, S. T.; Ruoff, R. S. *ACS Nano* **2008**, *2*, 572.
22. Bai, H.; Li, C.; Wang, X. L.; Shi, G. Q. *J. Phys. Chem. C* **2011**, *115*, 5545.
23. Yang, C. H.; Wang, M. X.; Haider, H.; Yang, J. H.; Sun, Y.; Chen, Y. M.; Zhou, J. X.; Suo, Z. G. *ACS Appl. Mater. Interface* **2013**, *5*, 10418.
24. Jeanie, L. D.; Robert, G. D.; David, J. M. *Biomaterials* **2004**, *25*, 3187.
25. Yang, J. S.; Zhou, Q. Q.; He, W. *Carbohydr. Polym.* **2013**, *92*, 223.
26. Liu, Y.; Zhao, J. C.; Zhang, C. J.; Guo, Y.; Cui, L.; Zhu, P.; Wang, D. Y. *RSC Adv.* **2015**, *5*, 64125.
27. Biji, A.; Cojazzi, G.; Panzavolta, S.; Rubini, K.; Roveri, N. *Biomaterials* **2001**, *22*, 763.
28. Rhim, J. W. *LWT-Food Sci. Technol.* **2004**, *37*, 323.
29. Russo, R.; Abbate, M.; Malinconico, M.; Santagata, G. *Carbohydr. Polym.* **2010**, *82*, 1061.
30. Deramos, C. M.; Irwin, A. E.; Nauss, J. L.; Stout, B. E. *Inorg. Chim. Acta* **1997**, *256*, 69.